第4章 ▶ 細胞機能の新しい制御法

① 組織幹細胞と糖鎖

■——はじめに

ヒトは約60兆個もの細胞から構成されているが，それらは相互に作用して組織・器官を形成し機能している．細胞は脂質と蛋白質からなる細胞膜で覆われた空間内で核内に共通のゲノムを有して存在しているが，組織・器官やその状態などによって俊敏に変化している．特にその制御には組織幹細胞が担っていると考えられている．たとえば消化管組織では基底部に存在する幹細胞から常に細胞が供給されることで新陳代謝を促す一方，外界と接している細胞は粘性の分泌蛋白質を産生し外敵の侵入を阻止したり内容物の効率的運搬や消化を促したりしながら，細胞間コミュニケーションをとりつつ細胞増殖/細胞死制御による組織の秩序を調節する細胞競合という機構が働く[1,2]ことで，組織としての恒常性が維持されている．こうした時空間的制御は主として蛋白質によってなされているが，その多くは翻訳後修飾として糖鎖が付加されており，蛋白質の局在，代謝，分泌に関与しているほか，細胞内情報伝達や細胞間接着など様々な生命活動の形成・維持において重要な役割を担っている(図1)．そこで本稿では組織の恒常性維持にかかわり，また再生医療の細胞ソースとしても考えられている組織幹細胞とその細胞機能を制御している糖鎖について，最近の研究の動向を含めて概説する．

1 組織幹細胞

1) 組織内幹細胞

組織幹細胞はそもそも組織内に存在していると考えられているが，実際に生体組織内のどの細胞が幹細胞であるかについてはっきりとしたことはほとんど明らかになっていない．その中で腸管上皮では基底部にある細胞が幹細胞として一定頻度で不等分裂して新たな細胞を供給して約3日ごとに上皮細胞が再生を繰り返すことが明らかになっている[3]．すなわち組織内では新たな細胞の産生，増殖，死が繰り返され，また酸化ストレスや外部刺激により損傷を受けた際の修復機構によって常に恒常性が維持されるように機能している．その原動力として働いていると考えられるのが組織内幹細胞といえる[4]．こうした幹細胞の存在や機能は，加齢とともに減少したり衰えたりするといわれ，各臓器の機能低下，すなわち老化を引き起こし，疾患発症のリスクを高めていると考えられる[5]．

2) 多能性を有する組織幹細胞

幹細胞を利用した細胞移植による再生医療は，すぐれた治療効果が得られる先端医療の一つとして注目されている．ここで使われる幹細胞は組織を酵素などで処理し特殊な条件下で培養することで自己複製能と多分化能を有する細胞として得られる．こうした幹細胞は受精卵からはじまる発生過程における組織構築の中で各組織内に存在している(図2)といわれ，実際 *in vitro* で培養可能となってきたことで様々な組織に存在していることが明らかになり，移植治療に利用可能な増殖・分化能力の高い前駆細胞や幹細胞が報告されている．それゆえに幹細胞移植による治療可能な対象疾患も増えつつある．その中で消化管組織は消化酵素を含む様々な分泌因子を放出する特殊な細胞群により構成されており，そうした機能を有する細胞

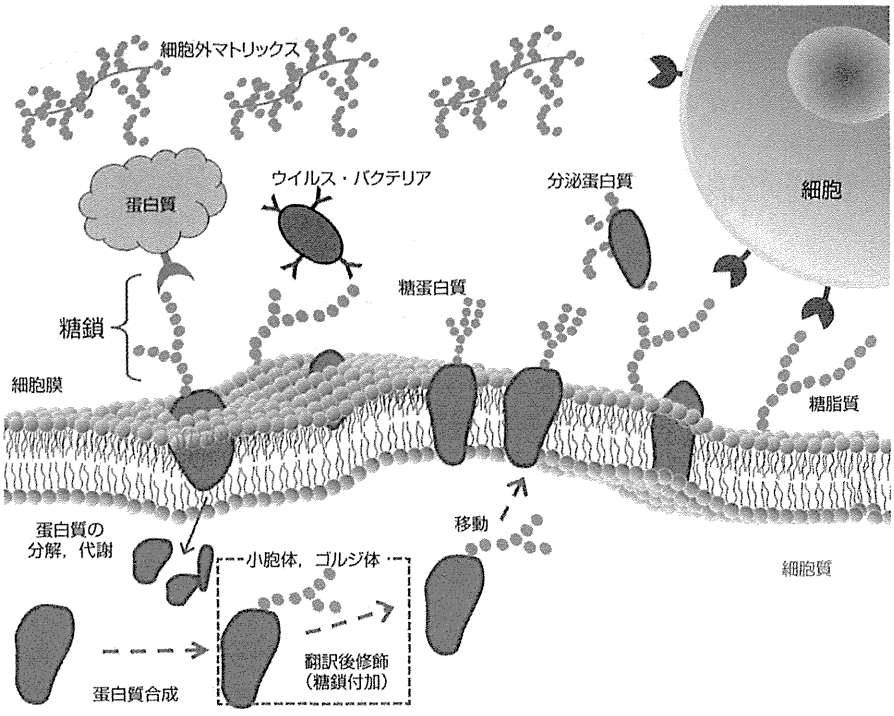

図1　細胞における糖鎖の役割

を移植したり機能修復を促進するような細胞を誘導したりすることは，かなりむずかしいといえる．より近い機能を有した細胞を採取するには消化管組織から幹細胞を採取するのがよいが，実際のところその主たる上皮系細胞を *in vitro* で培養し増やすことは，繊維芽細胞や間葉系幹細胞などと比べて容易ではない．しかも *in vivo* で示すような特性を維持した細胞を培養するとなると現状ではむずかしい．近年の培養技術開発の著しい進展のもと，ヒト消化管幹細胞の培養が可能となったとの報告もなされており[6,7]，さらには3次元培養技術の進展も著しいことから，今後消化管機能を有した幹細胞を採取，増やしていくことが可能となってくることが期待される．

3）幹細胞と老化，癌

初代培養細胞は継代を重ねていくと次第に増殖能が低下しついに停止に至る，いわゆる細胞老化が起こる．組織幹細胞も例外ではなく，継代によって分化能，増殖能を失っていくことが知られている．こうした状況は生体内でも起こる．消化管組織は細胞の代謝が最も早いといわれている組織の一つである．新たな細胞の産生は組織内幹細胞の細胞分裂によって起こるが，その分裂は他の組織よりも幹細胞の細胞老化を早めることになる．細胞は分裂ごとに染色体末端のテロメアの長さが短縮し，それがゲノム全体の不安定化につながり癌の発症を高めるといわれている[8]．実際種々の癌組織においてテロメアの短縮が観察されている[9,10]．こうした細胞老化は，組織幹細胞による移植医療に大きな壁となっている．これは，心臓や肝臓，脳神経系疾患などの治療に必要な多くの細胞を，採取可能な限られた組織から分化能を維持しながら増やすことがむずかしいからである．また得られた細胞がどの程度老化状態にあるかを見極めるのも現状ではそう簡単ではないこともある．細胞表面にある多様な糖鎖構造は，この老化に応じてどのように変化するかはこれまでに明らかにされていない．こうした未知の細胞の「今」の状態を反映する糖鎖情報を取得し，その機能を明らかにしていくことは，細胞の品質をより詳細にみる有力な知見を与え，今後に大きな役割を果たすと予想できる．

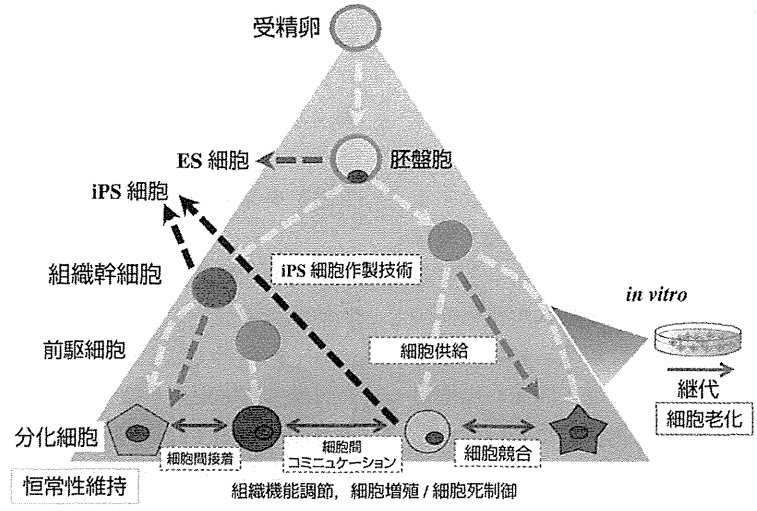

図 2 様々な幹細胞と組織恒常性の制御

2 糖鎖とマーカー

1) 糖鎖

糖鎖は，生体を構成する三つの鎖(核酸・蛋白質・糖鎖)の一つで，第 3 の生命鎖ともいわれている．多くの糖鎖は生体内において，糖脂質，糖蛋白質，プロテオグリカンなどの糖鎖複合体(複合糖鎖)として存在している．糖脂質や糖蛋白質は細胞膜外側に突きだすように糖鎖が存在し，主として細胞間認識にかかわっている．さらに糖蛋白質は，蛋白質本体の安定性や代謝に関与して細胞内機能の調節や，分泌因子としてシグナル分子としての役割を担っている．またプロテオグリカンは糖蛋白質の一種であるが，コア蛋白質を覆う一定様式で結合した糖鎖がその機能を制御している分子であり，細胞外マトリックスや基底膜などに存在し細胞や組織を支持する役割をしている．このように各組織を構成する細胞のほとんどが糖鎖で覆われ，細胞，組織の生理機能を維持している．それ故糖鎖は細胞や組織の状態(細胞社会)を反映するとされ，発生，分化，癌化，免疫など様々な生命現象に応じて変化すると考えられている(図 1)．このように時空間的制御における生命現象において細胞・組織の変化が糖鎖変化と関連し，バイオマーカーとして糖鎖の重要性が指摘されてきており，これまで多くの報告がなされ，実際の臨床での診断マーカーとして広く使われている．

2) 腫瘍マーカーと糖鎖

組織内の細胞は生理機能を果たすなかで様々な蛋白質を分泌している．ある種の癌化した組織内の細胞においては，正常時とは異なる糖鎖を有した蛋白質が分泌することが知られており，それが血液(血清)中に存在することで腫瘍のバイオマーカーとなる[11]．実際に臨床診断で利用されているマーカーの多くは糖鎖構造を認識している．癌細胞による糖蛋白質糖鎖の変化は癌の種類や発生場所によって特徴があるとされ，早期診断・治療へとつながり，また転移など再発予防にも役に立つとされる．さらに近年の複雑な糖鎖構造を解析する技術開発やレクチンの認識する糖鎖構造の特異性解析技術の進歩により，生命活動の維持にかかわる重要な役割を果たしている糖鎖が明らかになってきたという背景がある．血液(血清)中に存在する細胞・組織のわずかな変化を反映した異常な糖鎖構造をもった分泌糖蛋白質をとらえられるようになり，転移の有無や癌進行度に関係する糖鎖構造の解析が進めば，今使用されている腫瘍マーカー(CA19-9，STL，SLX，DuPanII，CA72-4 等)よりさらに精度の高い有用なマーカーが見出される可能性が期待できる．

3）疾患と糖鎖

現在，生体内での糖鎖を介した生命現象の分子機序が続々と明らかにされ，生命科学分野における糖鎖への注目度はますます高くなっている．これは，癌以外にも高齢社会をむかえ患者がますます増えていくと予想されているAlzheimer病などの認知症や脳心血管疾患，生活習慣病などに対して，疾患の早期発見・治療，さらに疾患発症の予防につながる，簡便でかつ低侵襲に体の状態をモニタリング可能なバイオマーカー開発への期待であり，糖鎖および糖鎖関連物質がその候補として医療への応用がさかんになっている[12]．

3 糖鎖と幹細胞

国内外ですでに臨床もしくは臨床研究において実施されている造血幹細胞移植や間葉系幹細胞移植による治療では，用いる細胞が細胞表面マーカーにより規定され安全性や有効性の指標となっている．そこで用いられるマーカーの中で糖鎖構造を認識している抗体も少なくない．これまで神経や心筋などの分化細胞を規定するマーカーは転写因子が多く，それでは細胞を生きたまま選別することができない．それゆえ細胞表面にある糖鎖がそれに変わる有力なマーカー候補となるのである．多能性幹細胞であるヒトES/iPS細胞はSSEA-3，SSEA-4[13]という糖脂質上の糖鎖構造やケラタン硫酸という硫酸化糖鎖を抗原とするTRA-1-60，TRA-1-81[14]に陽性であることが特徴的な形態とともに多能性獲得の指標となっている．胚性幹細胞(embryonic stem cell：ES細胞)や人工多能性幹細胞(induced pluripotent stem cell：iPS細胞)を用いた幹細胞移植医療が国内外で臨床研究段階に入っているが，いずれも分化誘導後移植前にこうしたマーカーを調べることで腫瘍(テラトーマ)形成能を有する未分化細胞の存在を調べる指標としても利用されている．また最近では細胞の糖鎖構造を網羅的に捉える糖鎖プロファイリングを行うことで，多能性幹細胞の未分化性判定や分化特性などが可能であることもわかった[15~17]．こうした解析から未分化多能性幹細胞特異的で，ライブイメージングが可能なレクチンも見出されている[18]．それゆえ特定の糖鎖ではなく全体の糖鎖プロファイリングによる細胞評価は多能性幹細胞を利用した再生医療に新たな評価軸として有用であるといえるだろう．より多様な組織幹細胞の指標も近い将来見出されるかもしれない．

■――おわりに

幹細胞を用いた再生医療が新たな局面を迎えている．国内外で臨床研究が行われており，その中で組織幹細胞から多能性幹細胞を利用した治療へ，患者の比較的少ない難治性疾患を対象にしたものから，より身近な疾患を対象とした治療へ，そして安全性の確認から有効な治療へと進んで行く段階にある．こうした中で移植した細胞が組織内でどのように作用して失った機能を再生するのかの研究も進んできている．これまで幹細胞側からの研究が中心となって失った機能をカバーする最適な細胞ソースを探索する研究が中心であったが，ここへ来て移植される組織側の環境要因も考慮する必要性がいわれている．外から入る細胞と受け止める細胞・組織間のいわゆる相性がよくなければ本来の機能を果たすことができないと考えられるからである．組織側には細胞のほかそれを支持する細胞外マトリックスが存在し，いずれも糖鎖で覆われている．そこでは細胞間接着やそれに基づく細胞内調整機能が重要な働きをすることを予想することは容易なことであり，そこに関与する糖鎖の役割がクローズアップされるのは必然の流れといえるだろう．これまで糖鎖は複雑で分析がむずかしいという概念を，最新の分析技術を駆使することで打ち破る期がまさに訪れているといえる．注目される再生医療を広く社会に還元するために必要な研究分野として大いなる進展が期待されるのがまさに糖鎖研究であるといえるだろう．

(豊田雅士，梅澤明弘)

◉文献

1) Amoyel M, et al.：Development **141**：988-1000, 2013
2) Hogan C, et al.：Int J Biochem Cell Biol **43**：496-503, 2011
3) 佐藤俊朗：生化学 **85**：743-748, 2013
4) Yamashita YM, et al.：Cold Spring Harb Perspect Biol **2**, a001313, 2010
5) Oh J, et al.：Nat Med **20**：870-880, 2014

6) Sato T, et al. : Nature **459** : 262-265, 2009
7) Sato T, et al. : Gastroenterology **141** : 1762-1772, 2011
8) Takubo K, et al. : Exp Gerontol **37** : 523-531, 2003
9) Takubi K, et al. : J Pathol **221** : 201-209, 2010
10) Aida J, et al. : Eur J Ca **46** : 430-438, 2010
11) Narimatsu H, et al. : FEBS J **277** : 95-105, 2010
12) Narimatsu H : Glycoconj J **31** : 403-407, 2014
13) Kannagi R, et al. : EMBO J **2** : 2355-2361, 1983
14) Badcock G, et al. : Cancer Res **59** : 4715-4719, 1999
15) Toyoda M, et al : Genes Cells **16** : 1-11, 2011
16) Tateno H, et al. : J Biol Chem **286** : 20345-20353, 2011
17) Tateno H, et al. : Stem Cells Trans Med **2** : 265-273, 2013
18) Onuma Y, et al. : Biochem Biophys Res Commun **431** : 524-529, 2013

PLOS | ONE

RESEARCH ARTICLE

Transcriptional Dynamics of Immortalized Human Mesenchymal Stem Cells during Transformation

Masao Takeuchi[1☯]*, Atsunori Higashino[2☯], Kikuko Takeuchi[1☯], Yutaro Hori[3,4], Kazuko Koshiba-Takeuchi[3], Hatsune Makino[3,5], Yoko Monobe[1], Marina Kishida[6], Jun Adachi[6], Jun Takeuchi[3,4,7‡], Takeshi Tomonaga[6], Akihiro Umezawa[5], Yosuke Kameoka[8], Ken-ichi Akagi[1‡]

1 Section of Laboratory Equipment, National Institutes of Biomedical Innovation, Health and Nutrition, Ibaraki-shi, Osaka, Japan, **2** Center for Human Evolution Modeling Research, Primate Research Institute, Kyoto University, Kyoto, Japan, **3** Division of Cardiovascular Regeneration, Institute of Molecular and Cellular Biosciences, The University of Tokyo, Tokyo, Japan, **4** Department of Biological Science, Graduate School Science, The University of Tokyo, Tokyo, Japan, **5** Department of Reproductive Biology and Pathology National Research Institute for Child Health and Development, Tokyo, Japan, **6** Laboratory of Proteome Research, National Institutes of Biomedical Innovation, Health and Nutrition, Ibaraki-shi, Osaka, Japan, **7** PRESTO, Japan Science and Technology of Agency, Tokyo, Japan, **8** Central Institute, A-CLIP Institutes, Chiba-shi, Chiba, Japan

☯ These authors contributed equally to this work.
‡ These authors also contributed equally to this work.
* takeuchim@nibiohn.go.jp

OPEN ACCESS

Citation: Takeuchi M, Higashino A, Takeuchi K, Hori Y, Koshiba-Takeuchi K, Makino H, et al. (2015) Transcriptional Dynamics of Immortalized Human Mesenchymal Stem Cells during Transformation. PLoS ONE 10(5): e0126562. doi:10.1371/journal.pone.0126562

Academic Editor: Kai Wang, University of Southern California, UNITED STATES

Received: September 12, 2012

Accepted: April 3, 2015

Published: May 15, 2015

Funding: This study was supported by the grant, No. 09158647, from the Ministry of Health, Labor, and Welfare of Japan. The funders had no role in study design, data collection and analysis, decision to publish, or preparation of the manuscript.

Competing Interests: The authors have declared that no competing interests exist.

Abstract

Comprehensive analysis of alterations in gene expression along with neoplastic transformation in human cells provides valuable information about the molecular mechanisms underlying transformation. To further address these questions, we performed whole transcriptome analysis to the human mesenchymal stem cell line, UE6E7T-3, which was immortalized with *hTERT* and human papillomavirus type 16 E6/E7 genes, in association with progress of transformation in these cells. At early stages of culture, UE6E7T-3 cells preferentially lost one copy of chromosome 13, as previously described; in addition, tumor suppressor genes, DNA repair genes, and apoptosis-activating genes were overexpressed. After the loss of chromosome 13, additional aneuploidy and genetic alterations that drove progressive transformation, were observed. At this stage, the cell line expressed oncogenes as well as genes related to anti-apoptotic functions, cell-cycle progression, and chromosome instability (CIN); these pro-tumorigenic changes were concomitant with a decrease in tumor suppressor gene expression. At later stages after prolong culture, the cells exhibited chromosome translocations, acquired anchorage-independent growth and tumorigenicity in nude mice, (sarcoma) and exhibited increased expression of genes encoding growth factor and DNA repair genes, and decreased expression of adhesion genes. In particular, glypican-5 (GPC5), which encodes a cell-surface proteoglycan that might be a biomarker for sarcoma, was expressed at high levels in association with transformation. Patched (Ptc1), the cell surface receptor for hedgehog (Hh) signaling, was also significantly overexpressed and co-localized with GPC5. Knockdown of GPC5 expression decreased cell proliferation,

suggesting that it plays a key role in growth in U3-DT cells (transformants derived from UE6E7T-3 cells) through the Hh signaling pathway. Thus, the UE6E7T-3 cell culture model is a useful tool for assessing the functional contribution of genes showed by expression profiling to the neoplastic transformation of human fibroblasts and human mesenchymal stem cells (hMSC).

Introduction

Neoplastic transformation of human fibroblasts and epithelial cells is thought to result from the sequential acquisition of genetic and/or epigenetic alterations in specific genes [1]. Much progress has been made in identifying and characterizing the genetic elements required to transform normal human cells [2–10]. Collectively, the results of these studies suggest that the transformation of human cells *in vitro* depends upon functional alterations in four to six genes. These alterations include changes in genes involved in telomere maintenance (to extend replicative lifespan), disruption of tumor suppressor pathways, and activation of oncogenes [2–10]. For example, the transformation of normal human fibroblasts requires the co-expression of *MYC*, *RAS*, and h*TERT* together with the functional loss of the *RB*, *PTEN*, and *p53* tumor suppressor pathways. However, a review by Duesberg and colleagues suggests that aneuploidy, in which a cell contains an abnormal number of chromosomes, is the primary cause of, and driving force behind, tumorigenesis: they state that aneuploidy results in an imbalance of gene expression, leading to the initiating event that initiates the transformation of normal cells [11].

An alternative explanation for the role of aneuploidy in tumorigenesis comes from mouse models harboring modifications in mitotic checkpoint genes. Studies of these mice have indicated that those showing reduced expression of mitotic checkpoint components, such as Bub1, BubR1, CENP-E, and Mad2, display an increased aneuploidy. In some mice, (CENP-E heterozygous mice, for example), reduced levels of *CENP-E* are associated with an increase in spontaneous tumorigenesis [12]. However, mice deficient in several spindle checkpoint–proteins, including BubR1, Bub1, and Bub3, display significantly increased level of aneuploidy without any increase in spontaneous tumorigenesis [13–15]. This indicates that even though aneuploidy is common in most human tumors, it is a promoter, rather than an initiator of tumor formation [16].

In addition, it is important to consider that distinct cell types show considerable differences in their susceptibility to transformation. Chromosomal changes in, or transformation of, human fibroblasts and hMSCs during culture can be caused not only by the introduction of the six genetic elements mentioned above, but also by the introduction of hTERT alone [17,18]. In addition, some hMSCs transduced with the hTERT gene show transformed phenotypes [17], but some are resistant [2,7,8,19]. Similarly, human embryonic stem cells continue to accumulate genetic and chromosomal changes during culture; these changes are similar to those observed in tumors [20]. The connection between genetic alterations and aneuploidy, both of which may induce transformation, remains unknown. However, the similarity between the final phenotype shown by different cells (i.e., transformed) suggests that the similar transformation programs, or an overlapping set of cancer-related genes, are involved.

By contrast, it is less clear how such genetic elements or aneuploids alter subsequent gene expression patterns influencing the progress of neoplastic transformation. To identify these genes and/or programs, we undertook a comprehensive analysis of gene expression changes in

an immortalized hMSC cell line, UE6E7T-3, and associated these changes with the phenotypic appearance, including chromosomal aberrations, during long-term culture.

Recently, we showed that UE6E7T-3 cells show the preferential loss of one copy of chromosome 13 upon prolonged culture, yielding cells with near-diploid aneuploidy [21,22]. However, at a population doubling level (PDL) of 110, near-diploid aneuploid cells do not display anchorage-independent growth. Here, we show that upon prolonged culture, these cells became near-triploid, began to proliferate at an increased rate, displayed anchorage-independent growth, and formed fibrosarcoma-like tumors in nude mice. Furthermore, we comprehensively examined the genetic and chromosomal alterations that might drive the transformation associated with these phenotypes and found an important factor, GPC5, which was overexpressed and contributed to cell proliferation at late stage.

Materials and Methods

Cell culture

The human mesenchymal stem cell line UE6E7T-3 (JCRB1136) was obtained from JCRB Cell Bank (Osaka, Japan), which entailed no ethical problems.

Imabayashi et al. isolated human mesenchymal cells (H4-3) from the bone marrow of a donor (91 years old, female) [23]. The UE6E7T-3 cell line, which was originally called 'ThMSC3', was immortalized from H4-3 cells using LXSN-E6E7 and LXSN-hTERT and deposited into JCRB Cell Bank (http://cellbank.nibio.go.jp/), which verified the quality of the cells. UE6E7T-3 cells were cultured in POWEREDBY10 medium (GP Biosciences Ltd., Yokohama, Japan, http://www.gpbio.jp/), as recommended by JCRB Cell Bank. POWEREDBY10 medium is widely available worldwide and the cells can also be cultured in DMEM containing 10% FBS. We confirmed that UE6E7T-3 cells also lost one of chromosome 13 in DMEM containing 10% FBS at near 100 PDL of culture period. Cells were seeded at a concentration of 5×10^3 cells/ml and cultured for 6–10 days, as described previously [21]. The population doubling level (PDL) was calculated as previously reported using the following formula: PDL = log (cell output/input)/log2 [22]. At the start of cultivation of this study, the PDL of UE6E7T-3 was 60. Further cultures consist of Stage I (PDL 60–90), Stage II (PDL 91–150), Stage III (PDL 151–230), and Stage IV (PDL 231–295). These four samples were named U3-A, U3-B, U3-C, and U3-DT, respectively. U3-DT cells (JCRB1136.01) at Stage IV (PDL 260) were deposited into the JCRB bank; the quality and ethics of the cells were verified by the bank.

Flow cytometry

Cells of Stage I (PDL 65 or 70), Stage II (PDL 92), Stage III (PDL 200) and Stage IV (PDL 252) were harvested with trypsin and suspended in 5% FBS-PBS at the concentrations of 1–2 x 10^6 cells/ml. 100 μl of each cell suspension was mixed with 5 μl of antibody diluted to 20 fold with 5% FBS-PBS. After incubation at 4°C for 20 min, cell suspension was washed 2 times with 5% FBS-PBS and was suspended with 500 μl of 4% paraformaldehyde–PBS. Data acquisition of 10,000 cells was performed using FACSCanto (BD). Analysis was performed using FlowJo software (TOMY Digital Biology). Antibodies used in this test were as follows, APC anti-CD34 (555824, BD), FITC anti-CD44 (IM1219U, Immunotech), FITC anti-CD45 (F0861, DAKO), RPE anti-CD73 (550257, BD), FITC anti-CD90 (F7274, DAKO), and RPE anti-CD105 (A07414, Immunotech). APC IgG1 (X0968, DAKO), FITC IgG1 (X0927, DAKO), RPE IgG1 (X0928, DAKO), and RPE IgG3 (731609, Immunotech) were also used as negative control.

Measurement of chromosome number and mFISH analysis

Measurement of chromosome number and mFISH analysis were performed as previously described [21]. Briefly, for mFISH analysis, metaphase chromosome spreads and the multicolor probe (mFISH-24Xcyte-kit, MetaSystems GmbH, Jena, Germany) were denatured with 0.07 N NaOH and hybridized at 37°C for 1–4 d. FISH images were captured and analyzed using a Zeiss Axio Imager microscope (Carl Zeiss Microimaging GmbH, Jena, Germany) and Isis mBAND/mFISH imaging software (MetaSystems GmbH).

Anchorage-independent growth (agar colony assay)

Between 125 and 1×10^5 cells were cultured in POWEREDBY10 medium containing 0.3% agarose (Invitrogen Co.) on 0.6% agarose for 21 days. Colonies of diameter >300 μm (including >100 cells) were counted [3].

Tumorigenicity assay

Tumorigenicity experiments were performed by subcutaneous (s.c.) or intramuscular injection (i.m.) of 1×10^7 U3-DT cells into BALB/cAJcl-nu/nu mice (Clea Japan, Inc., Tokyo, Japan) [24]. The protocols were approved by the Laboratory Animal Care and the Use Committee of the National Research Institute for Child and Health Development, Tokyo, Japan (approval numbers: 2003–002 and 2005–003). In the fourth week, the transplanted tissues were removed and embedded in paraffin blocks. Standard hematoxylin and eosin staining of paraffin-embedded tissue was performed for histological examination of tumorigenicity.

cDNA synthesis and whole-transcriptome sequencing

After subconfluent culture, 5×10^6–1×10^7 UE6E7T-3 cells at PDL 80 (Stage I), PDL110 (Stage II), PDL219 (Stage III) and PDL270 (Stage IV) were harvested. Each cellular total RNA from the four samples was extracted using QIAGEN RNeasy Mini Kit (Qiagen K. K., Tokyo, Japan). RNA samples were stored at −80°C until use. Poly-A RNA was used to select mRNA using the SOLiD RiboMinus Kit (Life Technologies, Gaithersburg, MD, USA). Following rRNA depletion, poly-A RNA was used to synthesize cDNA using the SOLiD Whole-Transcriptome Analysis Kit (Life Technologies) [25]. DNA sequencing (longest 50bp-reads) was carried out using SOLiD 3 PLUS System (Life Technologies) as described previously [26].

Mapping sequence data and RNA-Seq analysis

SOLiD sequence data were mapped on the NCBI/GenBank *Homo sapiens* genome sequence (hg19, http://hgdownload.cse.ucsc.edu/download.html#human). Quality control of these sequence data was performed using the CLC Genomics Workbench-v4.5 (CLC bio Japan, Inc. Tokyo, Japan). At least, 90% length and 80% similarity of the reference gene have been required in order to carry out the mapping of the sequenced reads to reference genome.

The Genomics Workbench yields gene expression values in units of "reads per kilobase of exon model per million mapped reads" (RPKM)

[27]. All sequence reads have been deposited to the DDBJ database of the National Institute of Genetics (http://www.ddbj.nig.ac.jp/), accession number DRA000533.

Cluster analysis and pathway analysis

Alignment to the NCBI *H. sapiens* genome sequence reference assembly (hg19) detected 33,565 genes from the RefSeq transcripts (S1 Table). Of these, 18,123 genes were expressed in mRNA extracted from U3-A cells. The expression of these genes was normalized to the

GAPDH expression in the same sample. We then filtered for fold changes of >2 or <0.5 in Relative Expression Value (REV; expression in U3-B,-C, or—DT divided by expression in U3-A), resulting in a set of 8,032 genes of U3-DT (S1A Fig). REV of GPC5 was the top value of all genes in U3DT cells. Of the top 10 REV, 6 genes (GPC5, CCDC3, COL4A5, ADCY8, CHRDL1, and PK1B) were also included in the top 10 REV of U3-C cells, but were not included in REV of U3-B cells. Genes with REV values between 0.5 and 2 were omitted from further analyses. Cluster and pathway analyses of the expression values of these 8,032 genes were performed using the Multi Experiment Viewer (MeV) software (http://www.tm4.org/mev) and IPA software (Ingenuity Systems, Inc., http//www.ingenuity.com/), respectively. "Diseases and Disorder" analysis was applied to REV of 8,032 genes in U3-DT cells by the IPA software and the most frequent result was "tumorigenesis". Furthermore, even if 18,123 genes were analyzed without utilizing a cut-off (0.5 to 2.0 REV), the same results were obtained. A total of 1,732 genes were analyzed, including 162 tumor-related genes identified from the literature and 1,570 genes detected by the IPA software (S1B Fig and S2 Table). We mainly classified 1,732 genes to 12 groups in accordance with information in the Gene database of NCBI.

qRT-PCR analysis using SYBR Premix EXTaq (Method A)

RNAs of U3-A (PDL 80, Stage I) or U3-DT cells (PDL 270, Stage IV) were extracted from 5×10^6 cells by the standard Trizol method using Sepasol RNAI Super G (Nacalai Tesque). RNA was reverse transcribed by ReverTra Ace qPCR RT Master Mix (Toyobo CO. LTD) and the cDNA subjected to qRT-PCR in a real-time PCR instrument (Thermal Cycler Dice Real Time Single System; Takara) with SYBR Premix EXTaq (Takara). GAPDH was used as the internal control. Primers used in the experiments were shown in (S1 Method).

siRNA treatment

U3-DT cells were seeded in 6-well tissue culture dishes (2×10^5 cells per well) and cultured in DMEM containing 10% FBS. The following day, cells were transfected with 100 or 200 nM of Accell Human GPC5 siRNASMARTpool or a non-targeting control siRNA [Thermo Scientific] in Accell siRNA Delivery Media containing 0.1%-FBS [Thermo Scientific] [28].

Cell proliferation assay

Cells were plated on 96-well tissue culture plates (2,000 cells per well) in 0.09 ml of DMEM containing 0.1% FBS. The cells were then used in CCK-8 assays (Dojindo Laboratories) according to the manufacturer's instructions. Briefly, 10 μl of CCK-8 reagent was added to each well and incubated at 37°C for 60 min. Cell proliferation was calculated on the indicated days by measuring the absorbance at 450 nm. The assay was performed in quintuplicate wells and each assay was performed at least three times.

Western blot analysis

siRNA-treated U3-DT cells were lysed in PTS buffer containing protease inhibitors and the protein concentration of each sample was adjusted to 10 μg/8 μl. Each sample was then analyzed by Western blotting with a rabbit MAb against anti-Glypican 5 (clone ab124886; Abcam) and HRP-linked anti-rabbit IgG-goat antibody (Cell Signaling Tech.) [29]. Colored marker (Protein MultiColor III) was purchased from BioDynamics Laboratory Inc.

Cell-cycle analysis

siRNA-treated cells were suspended in 0.1% FBS containing DMEM and 5×10^3 cells per well were cultured in a well of 98-wells plate for 5hr. Cells were treated with culture medium containing 20 μM 5-ethynyl-2'-deoxyuridine (EDU) for 30 min before they were harvested. The cells were then processed using the Click-iT plus EdU AlexaFluor 647 Imaging Kit (Invitrogen), stained with Hoechst 33342 and anti-Cyclin B1 rabbit IgG antibody and detected with Alexa 488-conjugated goat anti-rabbit IgG (Invitrogen; A-11008; 1:1000). Cell-cycle profiling of stained U3-DT cells was performed with an ImageXpress Micro (Molecular Devices).

Immunocytochemistry

Cells cultured on coverslips were washed in phosphate-buffered saline (PBS), fixed in 4% paraformaldehyde in PBS and then blocked with 1% BSA in PBS. The cells were stained with an anti-GPC5 antibody (R&D Systems, Inc.), or anti-Ptc1 antibody (LifeSpan BioSciences, Inc.), and Alexa Fluor 488 or 594 labeled secondary antibody (Molecular Probes, Inc.). The cells were then counterstained with DAPI and visualized using a fluorescence microscope (model BZ-9000; Keyence).

Results

Phenotypic characteristics of UE6E7T-3 cell line

This laboratory has previously demonstrated that aneuploidy, specifically the loss of one copy of chromosome 13, arises in the immortalized hMSC line UE6E7T-3 after prolonged culture [21,22]. We wished to investigate whether continuing culture after the appearance of aneuploidy would induce transformation of UE6E7T-3. To this end, we analyzed the phenotypic characteristics of the cells at various PDL (Fig 1). We monitored the growth characteristics of UE6E7T-3 cell line during long-term culture (Fig 1A). Alterations were observed in population doubling time (DT). DT was 40 hours at initial stage (Stage 1, PDL 65) and it slightly became longer at next stage (DT = 44, Stage II, PDL 120), and decreased to 28–22 hours afterward more than 150 PDL (Stage III, PDL 220 and Stage IV, PDL 252). Over the course of culture until PDL 252, UE6E7T-3 cells exhibited typical fibroblastic morphology with a uniform bipolar spindle shape, and no obvious morphological changes were observed (Fig 1B). Typical markers associated with hMSCs showed similar patterns at Stage I–IV, including markers that are expressed in hMSCs (CD44, CD73, CD90, and CD105) and those that are not (CD34 and CD45), although expression of CD90 and CD105 was slightly reduced at later stages (Fig 1C). In additionally, UE6E7T-3 cells can differentiate into adipocytes and osteocytes, an important characteristic of MSCs [21].

Changes in karyotype and neoplastic transformation during prolong cultivation

The growth rate at PDL 252 (population doubling time (DT) of 22 hours) was 2-fold higher than the rate at PDL 65 (DT: 40 hours). Distinct alterations in numerical and structural karyotypes appeared as PDL increased (Fig 2A and 2B). As shown in Fig 2A, nearly 90% of the cell population contained 46 chromosomes at PDL 62 (Stage I). By PDL 92, this proportion had decreased markedly to 17%, and a new population that contained 44–45 chromosomes had appeared. Between PDL 92 and PDL 147 (Stage II), cells were unstable and comprised several populations differing in karyotype: near-diploid, with 44–45 chromosomes (37–55%); diploid (2–17%); near-tetraploid, with 83–91 chromosomes (6–30%); and several minor populations. These populations were gradually replaced by near-tetraploid cells with 73–82 chromosomes

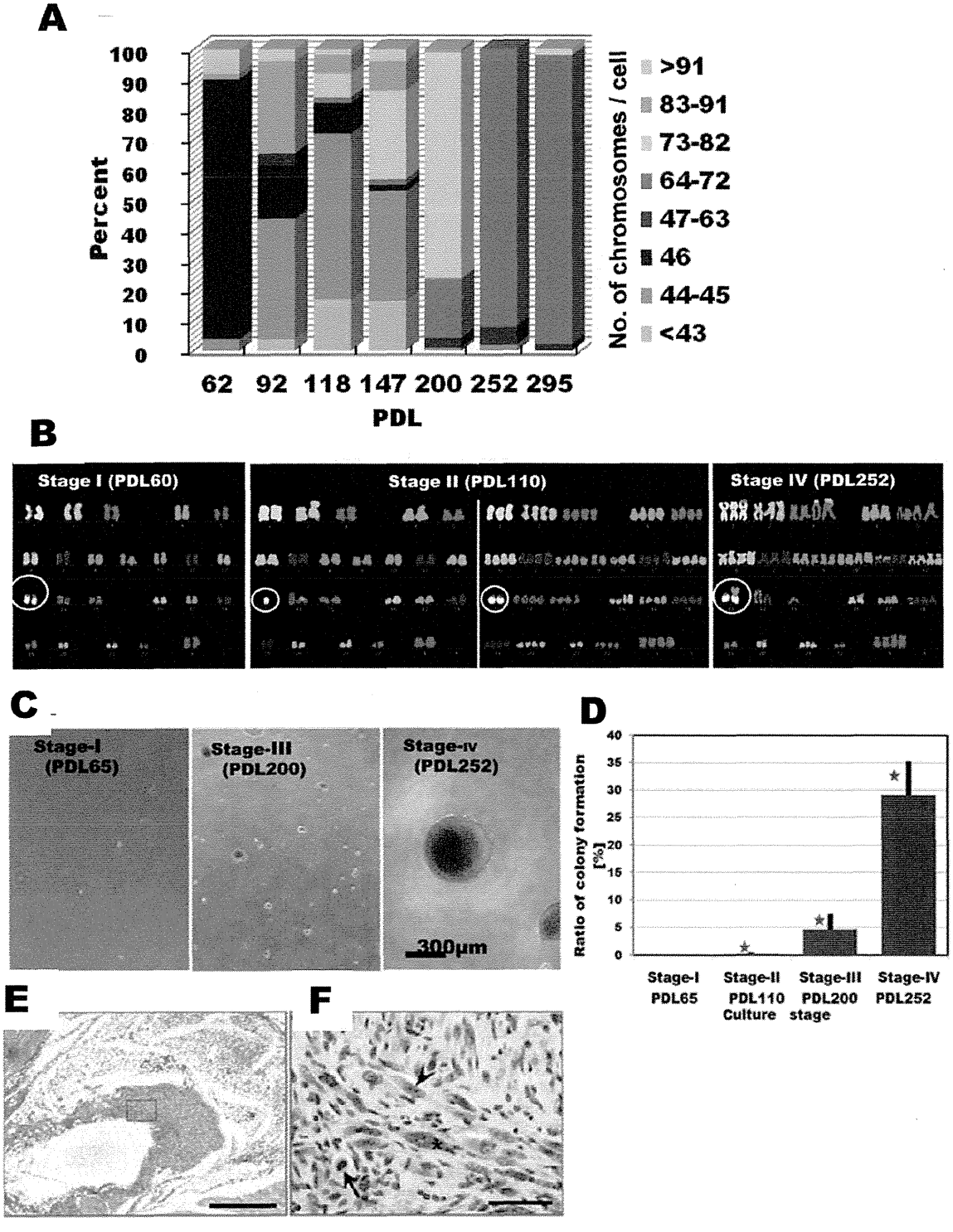

Fig 1. Phenotypic characteristics of UE6E7T-3 during long-term *in vitro* culture. (**A**) Growth curve. UE6E7T-3 cells were seeded at $5X10^3$ cells / ml in POWEREDBY 10. When cells were subconfluently grown, the cells were passaged with trypsin as shown in the text. After counting cell numbers, aliquot of the cultured cells was cultured continuously. (**B**) Phase-contrast images of UE6E7T-3 at four stages. Scale bar, 300 μm. (**C**) Flow cytometry. UE6E7T-3 cells (10,000 cells) were plotted. X-axis is fluorescence intensity. Y-axis is number of cell.

doi:10.1371/journal.pone.0126562.g001

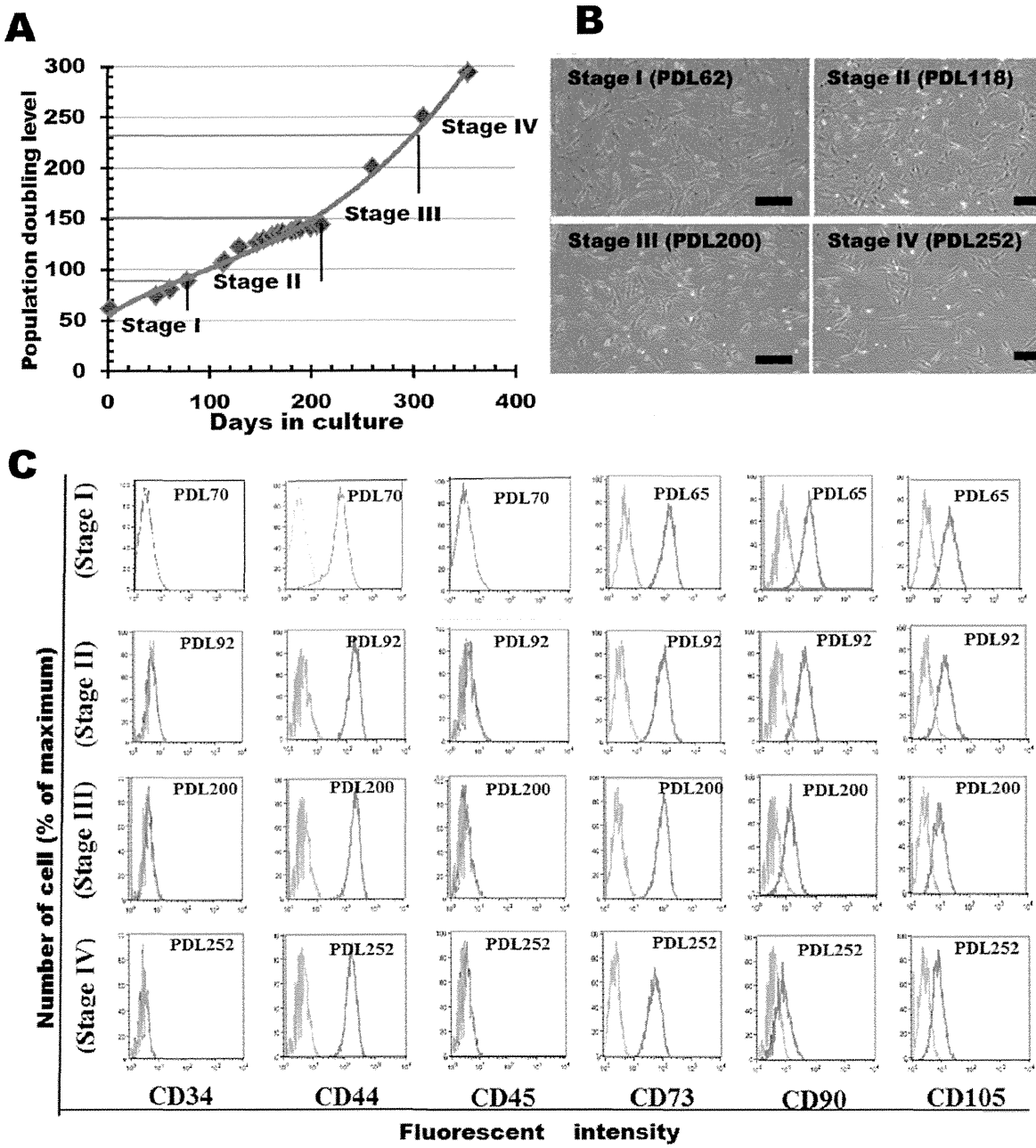

Fig 2. Phenotypic alterations of UE6E7T-3 during long-term culture. (**A**) Changes in chromosomal number at various culture stages. Chromosomes were counted by DAPI staining of 50–80 metaphase spreads at each PDL. Distribution pattern of cells at PDL 62, 92, 118, and 147 were rearranged from raw data from a previous report. (**B**) Multicolored fluorescence *in situ* hybridization (mFISH) karyotyping of UE6E7T-3 at three culture stages. Chromosome 13 is circled. (**C**) Colony formation in soft agar at three culture stages. (**D**) Graphical representation of the relative colony counts (expressed as percentages) at four culture stages. Colonies ≥300 μm in diameter were counted. Bars represent mean numbers of colonies of triplicates (percent + s.d.). ☆, $p < 0.01$. (**E**) Hematoxylin and eosin staining of invasive sarcoma following i.m. injection of U3-DT. Scale bar, 500μm. (Boxed area is magnified in D). (**F**) Magnification of transformed U3-DT in mouse muscle tissue. Dividing cells (arrow), cells containing two nuclear bodies (arrowhead), and cells containing increased chromatin (asterisk) indicate tumorigenesis. Scale bar, 50 μm.

doi:10.1371/journal.pone.0126562.g002

(72% at PDL 200, Stage III) and subsequently near-triploidy with 64–72 chromosomes. At further passages (PDL 252 and PDL 295, Stage IV); the population pattern remained stable with mostly near-triploid cells.

We next analyzed the structural karyotypes of UE6E7T-3 by mFISH. At PDL 60, cells exhibited a structurally normal diploid karyotype (Fig 2B, PDL60). By contrast, at PDL 92–147 there were several distinct populations (Fig 2B, PDL 110). Most of the near-diploid population, with 45 chromosomes, had lost one copy of chromosome 13 and one p-arm of chromosome 16 without translocations or insertions (n = 18 spreads; Fig 2B, PDL 110, left), whereas the population with 44 chromosomes had lost an additional chromosome (most often chromosome 21 or X) (n = 17 spreads). The near-tetraploid population consistently maintained two deletions of two copies of chromosome 13 and two p-arms of chromosome 16, with random loss of other chromosomes (Fig 2B, PDL 110, right), but exhibited few structural rearrangements. These results indicate that near-diploid aneuploidy arose through the loss of one or two chromosomes (one of which was chromosome 13) from a diploid cell; subsequently, near-diploid cells spontaneously became near-tetraploid via cleavage failure. After the formation of near-tetraploid, structural rearrangements such as translocations, insertions, and deletions occurred frequently, e.g., the fusion of chromosome 13 and chromosome 8, and the insertion of chromosome 13 into chromosome 14 (Fig 2B, PDL 252). This suggests that the deletion of chromosome 13 (formation of near-diploid aneuploidy) induces further chromosomal instability.

Neoplastic transformation of UE6E7T-3 cell line

Transformed cells lose contact inhibition, distinguishing them from normal cells, which cannot grow past confluence. To test the contribution of chromosomal instability (CIN) to transformation *in vitro* and *in vivo*, we examined the ability of UE6E7T-3 cells to form colonies in soft agar and tumors in immunodeficient mice. When UE6E7T-3 at various stages were seeded in soft agar, no anchorage-independent growth could be detected at early PDL (PDL 65 and 200), even after 4 weeks in culture. By contrast, a considerable number of anchorage-independent colonies were detected when PDL 252 cells were seeded in soft agar (Fig 2C and 2D). To determine whether this colony formation indicated tumorigenicity [12], cells at PDL 262 were injected subcutaneously or intramuscularly into immunodeficient nude mice. Four of the six mice injected with the PDL 262 cells formed sarcomas at the injection site after 4 weeks. Of the three mice injected intramuscularly, all formed sarcomas, although only one of the three mice injected subcutaneously did. Histological examination of the injected quadriceps femoris revealed these tumors to be invasive sarcomas, exhibiting spindle-shaped cells characteristic of fibroblasts (Fig 2E and 2F, arrow head). This observation indicates that UE6E7T-3 cells had undergone neoplastic transformation during long-term propagation in culture.

Gene expression profiling characterized at four stages of transformation *in vitro*

To date, the genes studied over the course of cellular transformation have been limited to a small number of genes encoding transcription factors (p53, E2F), cell-cycle regulators (p16, cyclins), oncogene products (RAS, MYC), and tumor suppressors (p53, RB). However, it is not obvious at which stage these factors act or how they play a causal role in advancing transformation. To obtain a comprehensive picture of changes in gene expression related to phenotypic alterations, we took representative samples at four stages during the progression of transformation (see Materials and Methods).

The expression profile from the Stage IV sample (U3-DT) was more similar to that of a Stage III sample (U3-C) than to that of the Stage II sample, U3-B (Fig 3A and S1A Fig). This

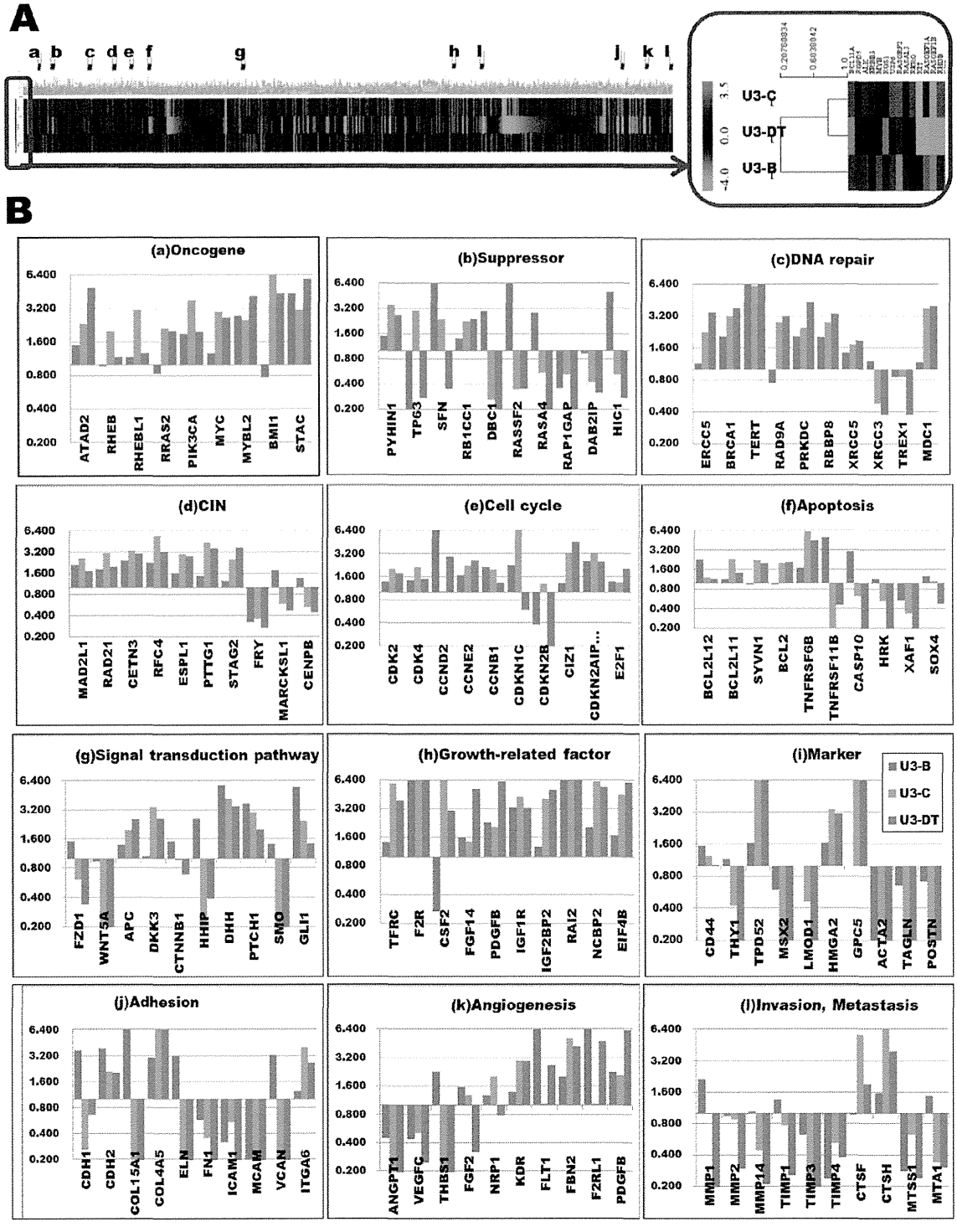

Fig 3. Alterations in expression of 1,732 selected genes. (**A**) *Heat-map representation of expression of 1,732 genes from samples* U3-B, U3-C, *and* U3-DT (taken from cultures at Stages II, III, and IV, respectively) compared with expression level in U3-A (from Stage I). Relative expression values (REV) from U3-A,-B,-C, and-DT are listed in S2 Table. (**B**) Functional classification of 1,732 genes and alterations in expression at three culture stages. All data described in this text is shown in S2 and S3 Tables. Blue, U3-B; orange, U3-C; red, U3-DT.

doi:10.1371/journal.pone.0126562.g003

observation suggests that important alterations in gene expression occur between Stages II and III.

Furthermore, to distinguish the genes that are important in the progression of phenotypic alterations from apparently random alterations, we filtered the 8,032 genes whose expression levels changed significantly (S1A Fig) and yield a subset of 1,570 genes by the IPA analysis (S1B and S1C Fig). The 1,732 genes (Fig 3A and S2 Table) were selected as described in Materials and Methods and were classified into 12 groups on the basis of pathways and cellular function (Fig 3A and 3B, and S2 and S3 Tables). REVs in each group are indicated relative to the control sample U3-A, which was derived from UE6E7T-3 (PDL 80) and exhibits a normal karyotype, typical fibroblastic morphology, and contact inhibition. Experimental results are also enumerated in S2 Table.

Oncogene and tumor suppressor gene expression

Genetic alterations commonly occurring in human tumors are often found in oncogenes and tumor suppressor genes. Alterations in the expression of such genes occurred in UE6E7T-3, and expression levels were markedly dependent on culture stage (Fig 3Ba and 3Bb). For example, oncogenes, *BMI1* and *MYC*, had low level expression at the early stage (Stage II), but were strikingly enhanced after Stage III. A similar pattern was also exhibited by other oncogenes. Tumor suppressor gene expression displayed an even more marked dependence on culture stage. Expression levels of *SFN*, *DBC1*, *RASSF2*, *DIRAS3*, *RASA4*, and *HIC1* were high at Stage II, but then rapidly decreased (Fig 3Bb, and S2 and S3 Tables). The marked decrease in *DBC1* (tumor suppressor gene) expression at Stages III and IV is in agreement with previous observations [30,31]. Although expression of *PRDM2*, *PYHIN1*, *RBBP4*, and *RB1CC1* (genes encoding activators of p53 or RB) were increased at Stages III and IV, relative expression levels of both *TP53* and *RB1* in U3-C and U3-DT were similar to those in U3-A, as were those of genes such as *PTEN* (Fig 3B, and S2 and S3 Tables).

DNA repair and chromosomal instability

When normal repair processes fail but apoptosis does not occur, irreparable DNA damage may occur during mitotic recombination events. This damage can take several forms, including double-strand breaks (DSBs) and DNA cross-linkages. In UE6E7T-3, the DNA repair processes appear to be constantly active at all stages, particularly at Stages III and IV, as evidenced by expression of genes encoding many kinds of DNA polymerases (*POLA1*, *POLE*), excision repair enzymes (*PRKDC*, *RBBP8*), nucleases, and checkpoint mediator proteins (*BRCA1*, *MDC1*) (Fig 3Bc, and S2 and S3 Tables).

A number of genes required for stepwise karyotypic alteration (a major source of chromosome instability) were also up-regulated during culture, as were genes associated with DNA repair, particularly at Stages III and IV. These included genes encoding components of the kinetochore and centromere (*NEK2*, *RAD21*, *SPC24*, and *STAG2*), participants in chromosomal segregation (*FOXMI*, *ESPL1*, and *PTTG1*), motor proteins involved in chromosome positioning (*KIF4A*, *KIF2C*, *CENPE*, and *CENPF*), and regulators of cytokinesis (*PRC1*). Overexpression of *MAD2L1* and *PTTG1* (securin) has been observed in several tumor types [32,33]. Recently, Schvartzman and colleagues demonstrated direct evidence for inhibition of the p53 or Rb pathways leading to up-regulation of *MAD2L1*, and that this up-regulation is required for generating chromosome instability [34]. Our observations of the inactivation of Rb and p53 by HPV-16 E6/E7, generation of chromosome instability, and *MAD2L1* overexpression strongly support their result. In addition, down-regulation of *FRY* or *CENPB* may also contribute to chromosome instability through de-regulation of chromosome alignment and

formation of the spindle and kinetochore. All up-regulated chromosome instability genes in UE6E7T-3 are among the 70 genes best correlated with total functional aneuploidy in several cancer types [35].

Cell cycle

Generally, one cell cycle is completed within 20–100 hours, most of which is spent in the G1 phase [36]. Mechanisms regulating the cell cycle are common to all cells and are driven by three types of factors: cyclin-dependent kinases (CDK), cyclins, and cyclin-dependent kinase inhibitors (CKI). As shown in Fig 3Be, and S2 and S3 Tables, CDK-related genes (*CDC25C*, *CDK2*, *CDK4*, *CDC2L6*, *CDC2*, and *CDK2AP2)* and cyclin genes (*CCND2*, *CCNE2*, and *CCNB1*) were up-regulated at all culture stages, whereas CKI-encoding genes such as *CDKNIC* (p57), *CDKN2B* (p15), *CDKNIA* (p21), *CDKN2A* (p16), and *CDK2AP1* were down-regulated at all stages. These alterations in cell-cycle gene expression resulted in an uncontrolled increase in proliferation. Gene expression profiles at four stages of culture (PDL 80, 110, 219, and 270) are shown in Fig 4. As a control, we used U3-A (PDL 80). Marked differences in gene expression patterns between U3-B and U3-C were observed. In U3-C (Stage III), we also observed high expression of *MYC*, *MYBL2* (CDK-activating gene), *BMI1* (p16-suppressing gene), *CIZ1*

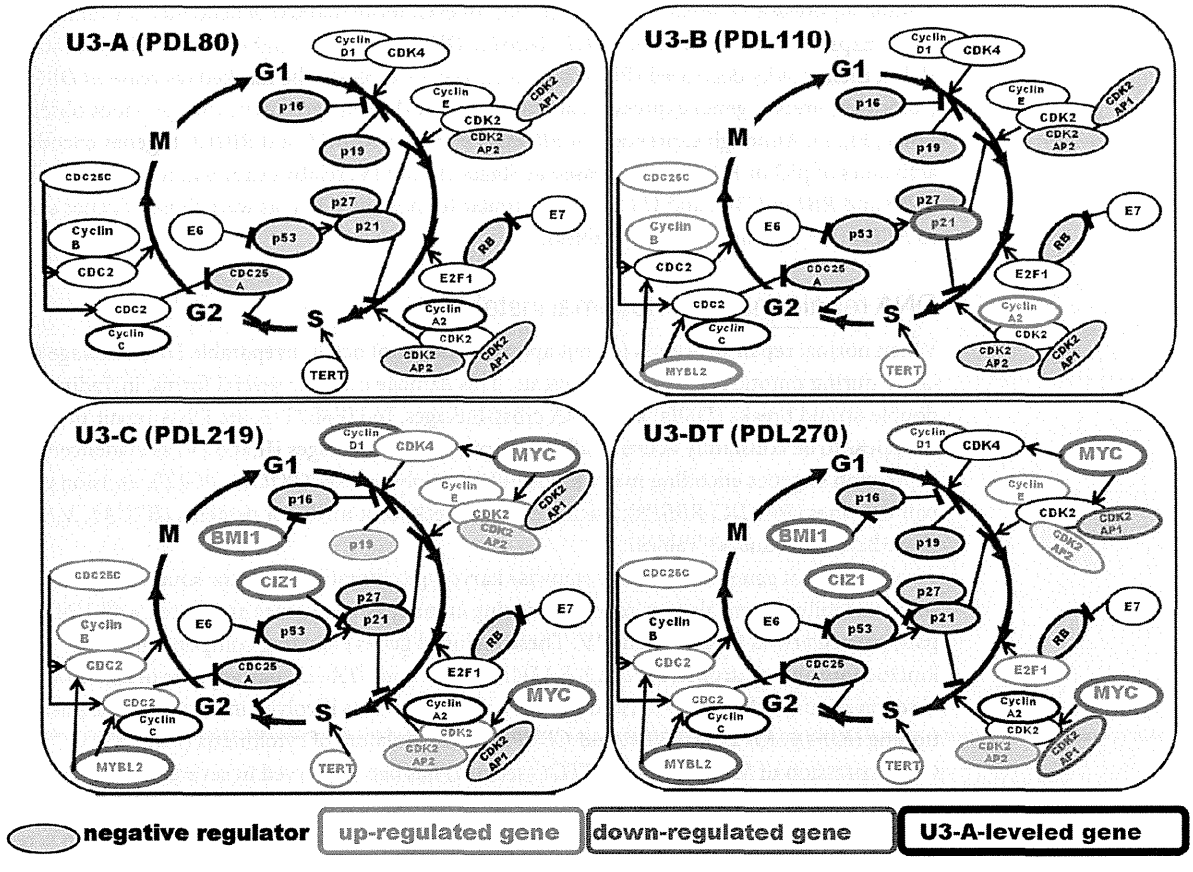

Fig 4. Gene expression in the cell-cycle pathway during long-term culture of UE6E7T-3. U3-A, U3-B, U3-C, and U3-DT are samples from culture Stages I, II, III, and IV, respectively. Changes in gene expression relative to the level in U3-A (Stage I) are shown. Red characters, up-regulated; purple characters, down-regulated; black characters, U3-A (control) level; Blue fill, negative regulator. Genes with REV >2 or <0.5 are indicated as up- or down-regulated, respectively.

doi:10.1371/journal.pone.0126562.g004

(p21-inhibiting gene, [37]), and *ATAD2* (cofactor gene of MYC) [38], in addition to increased gene-expression of CDKs and cyclins. These changes were concomitant with a strong depression of CKI-encoding gene expression. Together, these observations suggest that these alterations play a crucial role in rapid proliferation.

E2F1, which encodes a transcriptional activator, was also expressed at higher levels at late stages. The expression of *E2F1* is intimately regulated by RB. Functional inactivation of the RB pathway in this cell line leads to *E2F1* overexpression, which may be correlated with rapid cell proliferation. Another factor contributing to the higher rate of proliferation is the functional loss of p53 checkpoint pathways. Together, these alterations explain the decrease in U3-C doubling time, which dropped to 28 hours from 44 hours in U3-B.

Apoptosis

Resistance to apoptosis is one of the hallmarks of cancer. At Stage II, apoptosis-inducing genes such as *TNFRSF11B* and *CASP10* were expressed at high levels, but as in the case of tumor suppressor genes, expression rapidly decreased. By contrast, expression of apoptosis-suppressing genes (*TNFRSF6B*, *BCL2*, etc.) was enhanced at later stages (Fig 3Bf, and S2 and S3 Tables).

Signaling pathways and growth factors

Extracellular signaling molecules, such as growth factors, activate specific receptors on the target cell membrane, activating second messengers, and eventually elicit a physiological response. As shown in Fig 3Bg, and S2 and S3 Tables, striking alterations in gene expression were observed only in the Hedgehog (Hh) signaling pathway (*DHH*, *PTCH1*, *SMO*, and *GLI1*); however, some of these genes were down-regulated at later stages. By contrast, genes encoding Wnt signaling factors (*FZD1*, *WNT5A*, *APC*, and *CTNNB1*) are not likely to be implicated in the transformation of UE6E7T-3 cells.

Unregulated expression of growth factors, cytokines, receptors, and signaling components is linked to developmental abnormalities and a variety of chronic diseases, including cancer. In UE6E7T-3, such genes were considerably up-regulated, especially at later stages (Fig 3Bh, and S2 and S3 Tables). The expression levels of *IGF2BP2*, *RAI2*, *SLC25A27*, *NCBP2*, and *EIF4B* were greatly enhanced, as is the case in tumor development. *TFRC*, a marker of human pancreatic cancer [39], was also expressed at a high level, as was *F2R*, which encodes a G-protein-coupled receptor. By contrast, expression levels of genes encoding chemokines or interleukins and their receptors were undetectable.

Lineage markers and adhesion-associated genes

Genes encoding markers of mesenchymal cells (CD44, CD73, CD90, and CD105) were expressed in U3-DT at levels similar to those in U3-A (Fig 1C). Tumor-marker genes (*HMGA2*, *TPD52*, and *GPC5*) were overexpressed in U3-C and U3-DT (Fig 3Bi, and S2 and S3 Tables). U3-A has the potential to differentiate into several types of cell, including adipocytes and osteoblasts [21]. Gene expression of markers characteristic of these cell types was down-regulated in U3-DT cells (*ACTA2*, *MSX2*, *CNN1*, *TAGLN*, *LMOD1*, and *POSTN*).

Expression of adhesion-related genes was strongly suppressed in U3-C and U3-DT, with the exception of *COL4A5*, a member of the collagen family (Fig 3Bj, and S2 and S3 Tables). E-cadherin (product of *CDH1*) is one of the most important molecules in cell-cell adhesion in epithelial tissue. *CDH1* expression was markedly reduced in U3-C (Fig 3Bj, and S2 and S3 Tables). Suppression of *CDH1* expression is one of the primary molecular events responsible for dysfunction in cell-cell adhesion, such as that which occurs in tumor progression. On the other hand, N-cadherin (*CDH2*) expression remained high. Other adhesion molecules were also

expressed at low levels comparable to those in U3-A, as observed in tumor cells. Expression levels of integrins, receptors that mediate attachment of cells to extracellular components such as collagen and fibronectin, were normal; however, collagen expression reduced considerably with tumorigenic progression. These results suggest that reduced expression of these adhesion molecules plays an important part in promoting invasion into surrounding stroma.

Angiogenesis, invasion, and metastasis

Oxygen and nutrients supplied by vasculature are crucial for cell function and survival. Beyond a certain size, tumors induce blood vessel growth (angiogenesis) by secreting various growth factors, thereby allowing the tumor to obtain oxygen and essential nutrients *in vivo*. In UE6E7T-3, genes encoding major contributors to angiogenesis (*TEK*, *VEGFC*, *FGF2*, and *ANGPT1*) were expressed at remarkably low levels, although the expression of genes encoding their receptors (*KDR*, *FLT1*) was high (Fig 3Bk, and S2 and S3 Tables). Another major contributor to angiogenesis is matrix metalloproteinase (MMP1, MMP2, MMP3, and MMP14). These proteases were also expressed at low levels, as were the MMP inhibitors (TIMP1, TIMP3, and TIMP4) (Fig 3Bl, and S2 and S3 Tables).

Similar low levels of expression were observed in invasion- and metastasis-related genes. Cell-cell and cell-matrix adhesion molecules play an important role in cell migration. E-cadherin, which is considered an important suppressor of invasion and metastasis, rapidly decreased in gene expression at Stage III (Fig 3Bj, and S2 and S3 Tables). This reduction is likely to represent a key step in the acquisition of invasive properties. Furthermore, integrin family genes (*ICAM1*, *ICAM2*, *ICAM5*, and *VCAM1*) were also expressed at low levels (Fig 3Bj, and S2 and S3 Tables). These results suggest that even U3-DT may still be in the earliest stages of tumorigenesis. Alternatively, in terms of angiogenesis-, invasion- and metastasis-related gene expression, tumorigenesis in fibroblastic cells may differ from that of epithelial cells.

Validation of RNA-Seq

To evaluate of RNA-Seq analysis, we chose 29 genes at Stage IV in each pathway identified by RNA-Seq for qRT-PCR analysis (Fig 5). The expression pattern of the genes determined by qRT-PCR analysis is similar to the results of RNA-Seq analysis, although slight differences in expression level were detected between two methods. In addition, to confirm the accuracy of RNA-Seq data we compared the expression levels of 41 samples according to RNA-Seq and qRT-PCR analyses, including 29 genes at Stage IV analyzed by Method A and 4 genes at Stage II-IV analyzed by Method B (S1 Method), and obtained a high concordance (Spearman's rank correlation coefficient, R = 0.76) between these two sets of data (S1 Method and S1 Fig). A coefficient of 0.76 corresponds to a significance level of slight less than 0.1%. This indicated that our RNA-Seq could reliably measure gene expression differences.

GPC5 expression affects UE6E7T-3 cell proliferation

A unique pattern of gene expression was observed in UE6E7T-3 cells; GPC5 was overexpressed at the late stage of long-term culture. To assess whether this overexpression affected the proliferation in U3-DT cells, we examined the effect of GPC5 knockdown. Knockdown of GPC5 by GPC5 siRNA (SMARTpool siRNA) was confirmed by Western blot analysis (Fig 6A), and resulted in significant inhibition of proliferation of U3-DT cells compared with that in cells infected with control non-target siRNA (Fig 6B). These results show that overexpression of GPC5 stimulates the proliferation of U3-DT cells.

The proliferation rate of cells treated with target-specific siRNAs was comparable to the rate of cells treated with a non-targeting siRNA control, but the growth curve had lag phase at the

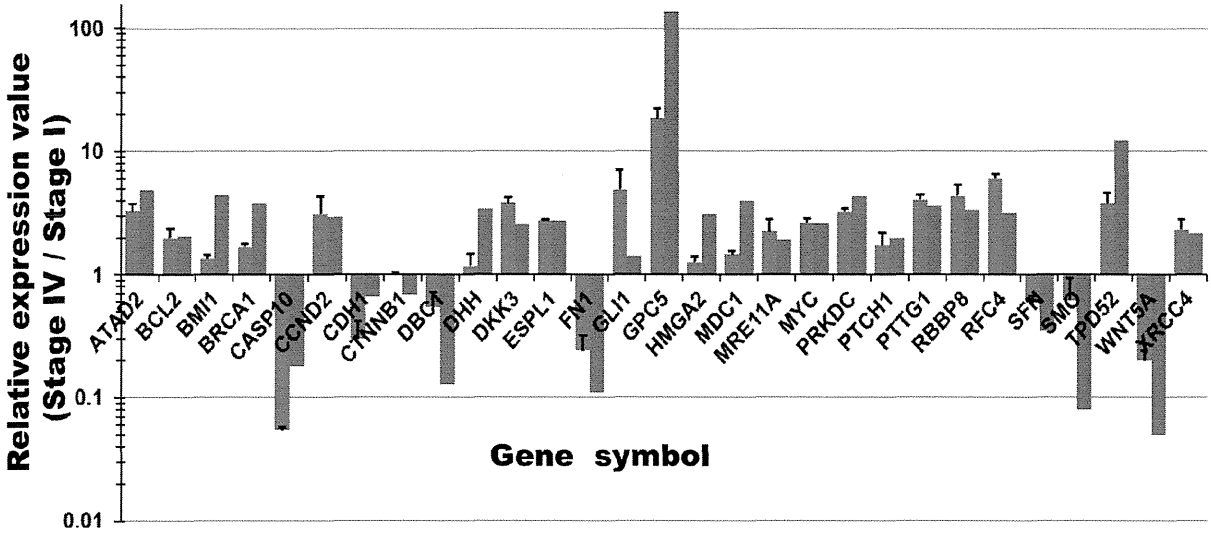

Fig 5. Comparison of RNA-Seq and qRT-PCR. Results of qRT-PCR analysis of remarkable genes at Stage IV are shown as the relative expression ratio (blue) compared to those of the RNA-Seq analysis with whole transcriptome sequencing (red). Bar, standard error.

doi:10.1371/journal.pone.0126562.g005

initial stage (Fig 6B). To examine which phase in the cell cycle is affected by the target-specific siRNA, we used an ImageXpressMicro analyzer (Molecular Devices). As shown in Fig 6C, treatment with specific siRNAs resulted in an increase of cell numbers in G1 phase and slight decreases in S, G2 and M phases, indicating that the decreased proliferation induced by siRNA is due to the retention of cells in G1. Cell-cycle distribution analysis did not reveal any cells in the sub-G1 phase following siRNA treatment and we did not observe any cells with apoptotic morphology.

Li et al. [28] reported recently that GPC5 localizes to the primary cilium in rhabdomyosarcoma (RMS) cells and promotes cell proliferation by binding to Ptc1, the cell-surface receptor for Hh signaling. Our RNA-Seq and qRT-PCR analyses showed that Ptc1 is significantly upregulated in U3-DT cells. Therefore, to investigate the interaction between GPC5 and Ptc1, we examined the localization of endogenous GPC5 and Ptc1 in U3-DT cells with antibodies against GPC5 and Ptc1. Although both GPC5 and Ptc1 antibodies weakly and diffusely stained U3-A cells (data not shown), strong staining of GPC5 was detected at the same region of concentrated Ptc1 staining (Fig 6D). This fluorescence staining pattern is similar to the endogenous localization of GPC5 in the cilia of RMS cells [28] and of Ptc1 in the cilia of NIH 3T3 cells [40]. This finding suggests that GPC5 interacts with components of the Hh signaling pathway.

Discussion

This study shows that the hMSC line, UE6E7T-3, immortalized with the *hTERT* gene in combination with the HPV-16 E6/E7 genes, gradually transformed during prolonged culture. The HPV-16 E6/E7 gene products, the E6 and E7 proteins, abrogate repression of the cell cycle through their associations with p53 and pRb, respectively [41]. In parallel with acquisition of increased tumorigenicity, numerous alterations in gene expression occurred spontaneously with culture passage. These alterations are similar to previous data, which MSCs derived from $p21^{-/-}p53^{+/-}$ mice completely lost p53 expression after *in vitro* long-term culture and formed sarcomas *in vivo* [42] and muline MSCs derived osteosarcoma cells in consequence of aneuploidization and genomic loss of Cdkn2 [43]. Our comprehensive gene expression analysis